the optimal trajectory was then performed twice giving the slight differences shown in Fig. 2. However, the difference between the two flight tests is less than the difference between the flight tests and the computation, showing the excellent skills of the pilot in following the prescribed trajectory. Further, it was very encouraging to see that the theoretically predicted time reduction of 28% was so closely reproduced in the flight test, which gave a time reduction of approximately 30%.

## Conclusions

It was expected that the ability of the pilot to follow the desired trajectory would be the main uncertainty in the test. However, the present case and further testing currently in progress suggest that it is indeed quite possible to follow even quite complex trajectories with a bit of training in a simulator. However, the longer term goal is to compute the desired trajectory in close to real time and then let an autopilot fly the trajectory significantly reducing pilot workload.

Apart from the uncertainty in engine performance already mentioned, a much more significant uncertainty appears to be the atmospheric model. Standard procedure calls for using the ISA, possibly modified with a constant temperature shift. However, investigating the atmospheric variation as a function of altitude during the tests showed that the conditions are not often well represented by a model involving a constant temperature shift from the ISA. Instead, the model should be based on local information, where temperature and static pressure are given as functions of geopotential altitude. This information is available from the weather service at F10 but is not yet implemented in the computational model.

A significant computational difficulty that often appears when solving trajectory optimization problems is the robustness of the solution method. The optimization problem [Eqs. (11) and (12)] is highly nonlinear, and the algorithm does in practice not always converge to a local optimum. A particular case where the algorithm may fail is when the local quadratic programming model of Eqs. (11) and (12), used to define the next approximation to the solution, does not have a feasible solution even though the original nonlinear problem has a solution. The sequential quadratic programming method[9] used here has the facility to deal with this case but it does not always work. Further difficulties arise when there indeed is no feasible point to the constraints (12). Deciding whether or not there exists a feasible solution is a problem that is at least as difficult as solving the optimization problem itself.

Despite the occasional difficulties described, it is still possible to solve quite general performance optimization problems using the method described. Problems such as a brief acceleration or a climb problem, as well as maximum range problems, can be solved using the same optimization method. Furthermore, the limited flight testing performed also suggest that the results may be quite useful in practice.

## Acknowledgments

This project is financially supported by the Swedish Defense Materiel Administration (FMV) Project 61969-LB104302. The author is most grateful for the support provided by the staff of FMV:FlygFT, in particular Martin Näsman. Special thanks are also due to the staff at the Swedish Air Force base F10 in Ängelholm, especially Dan Eriksson and Axel Nilsson, who made the flight tests possible. The author is also most grateful for the support of Philip Gill at the University of California, San Diego, and Walter Murray and Michael Saunders at Stanford University.

## References

[1]Bryson, A. E., Jr., and Desai, M. N., "Energy-State Approximation in Performance Optimization of Supersonic Aircraft," *Journal of Aircraft*, Vol. 6, No. 6, 1969, pp. 481–488.

[2]Hargraves, C. R., and Paris, S. W., "Direct Trajectory Optimization Using Nonlinear Programming and Collocation," *Journal of Guidance, Control, and Dynamics*, Vol. 10, No. 4, 1987, pp. 338–342.

[3]Gill, P. E., Murray, W., Saunders, M. A., and Wright, M. H., "User's Guide for NPSOL (Version 4.0)," Rept. SOL 86-2, Dept. of Operations Research, Stanford Univ., Stanford, CA, 1986.

[4]Brenan, K. E., "Differential-Algebraic Equations Issues in the Direct Transcription of Path Constrained Optimal Control Problems," Aerospace Rept. ATR-94(8489)-1, The Aerospace Corp., El Segundo, CA, Dec. 1993.

[5]Gill, P. E., Murray, W., and Saunders, M. A., "Large-Scale SQP Methods and Their Application in Trajectory Optimization," Dept. of Mathematics, Rept. NA 93-3, Univ. of California, San Diego, CA, 1993.

[6]Shi, Y. Y., Nelson, R., Young, D. H., Gill, P. E., Murray, W., and Saunders, M. A., "The Application of Nonlinear Programming and Collocation to Optimal Aeroassited Orbital Transfer Trajectory," AIAA 92-0734, Jan. 1992.

[7]Betts, J., "Experience with a Sparse Nonlinear Programming Algorithm," *Large-Scale Optimization with Applications*, edited by A. Conn and F. Santosa, Vol. 93, Inst. for Mathematics and its Applications, Springer, Berlin, 1997, pp. 53–72.

[8]Seywald, H., and Kumar, R., "Some Recent Developments in Computational Optimal Control," *Large-Scale Optimization with Applications*, edited by A. Conn and F. Santosa, Vol. 93, Inst. for Mathematics and its Applications, Springer, Berlin, 1997, pp. 203–234.

[9]Gill, P. E., Murray, W., and Saunders, M. A., "Users Guide for SNOPT 5.3: A FORTRAN Package for Large-Scale Nonlinear Programming," Dept. of Mathematics, Rept. NA 97-X, Univ. of Calfornia, San Diego, CA, 1997.

# Transonic and Low-Supersonic Aerodynamic Analysis of a Wing with Underpylon/Store

Dong-Hyun Kim* and In Lee†
*Korea Advanced Institute of Science and Technology, Taejon 305-701, Republic of Korea*

## Introduction

MODERN multipurpose military aircrafts are often equipped with several types of wing-mounted external stores. Generally, external stores are placed on the undersurface and tip of aircraft wing as extra fuel tanks or weapons such as missiles, bombs, rockets, and gun pods. In the transonic and low-supersonic speeds there is strong shock interference between the wing and the pylon/store, which causes a severe vibration of the aircraft wing such as flutter, limit cycle oscillation, and buffet, etc. If the aircraft is under the continuous vibration condition as just mentioned, there are critical structural and fatigue damages of wing structures. So, the correct prediction of instability such as flutter is essential. A typical flutter analysis requires several unsteady aerodynamic computations. In addition, such computations using the method of computational fluid dynamics are quite expensive in the transonic and low-supersonic regime. Therefore, the development of efficient and accurate computational codes for the unsteady aerodynamics is very important for the flutter analysis.

The detailed wind-tunnel experiments for the F-5 fighter wing had been conducted at the National Aerospace Laboratory of the Netherlands (NLR) under the sponsorship of the U.S. Air Force.[1] It could be shown from NLR's experiments that there was clearly a strong influence of the underpylon/store on the steady and unsteady transonic aerodynamics. From the 1970s there were great efforts to develop efficient unsteady aerodynamic codes based on the three-dimensional transonic small-disturbance (TSD) theory. As the results of previous researches, the famous and very efficient codes such as ATRAN3S[2,3] and CAP-TSD[4,5] have been developed and verified for several application cases.

Received 10 August 1999; revision received 7 September 1999; accepted for publication 7 September 1999. 

*Graduate Research Assistant, Department of Aerospace Engineering, 373-1, Kusong-dong, Yusong-gu. Member AIAA.

†Professor and Chairman, Department of Aerospace Engineering, 373-1, Kusong-dong, Yusong-gu. Senior Member AIAA.

The present TSD3KR code, which is also based on the transonic unsteady small-disturbance theory developed and extended by the present authors, can effectively analyze the aerodynamics of aircraft wings with control surfaces and external pylon/stores. This paper is to introduce the additional aerodynamic results in the transonic and low-supersonic flow region, which have not yet been analyzed and compared in other references, and to show the refined schematic grid system used in the present TSD3KR code. The steady and unsteady transonic results were compared with wind-tunnel results available for the F-5 wing. Effects of the understore on the steady and unsteady transonic flow of F-5 wing are also studied. The present paper briefly describes the numerical analysis and comparison results with available experimental data. These results are in a good agreement with the National Aeronautical Laboratory experimental steady and unsteady pressure data. However, there are some differences in the region of strong shock interaction between wing and underpylon/store.

## Computational Background

The TSD3KR code is a finite difference computer code such as ATRAN3S and CAP-TSD that solves the modified TSD equation. The TSD potential equation transformed to the computational domain using the modified shearing transformation[2] can be written in the strong conservation form as follows:

$$
\begin{aligned}
&-\frac{\partial}{\partial \tau}\left(\frac{M^2}{\xi_x}\phi_\tau + 2M^2\phi_\xi\right) + \frac{\partial}{\partial \xi}\Bigg[(1-M^2)\xi_x\phi_\xi + F\xi_x^2\phi_\xi^2 \\
&\quad + G(\xi_y\phi_\xi + \phi_\eta)^2 + \frac{\xi_y}{\xi_x}(\xi_y\phi_\xi + \phi_\eta) + H\xi_y\phi_\xi(\xi_y\phi_\xi + \phi_\eta)\Bigg] \\
&\quad + \frac{\partial}{\partial \eta}\left[\frac{1}{\xi_x}(\xi_y\phi_\xi + \phi_\eta) + H\phi_\xi(\xi_y\phi_\xi + \phi_\eta)\right] + \frac{\partial}{\partial \varsigma}\left(\frac{1}{\xi_x}\phi_\varsigma\right) = 0
\end{aligned}
\tag{1}
$$

where $M$ is a freestream Mach number, $\phi$ is the small disturbed potential, and $\tau$ is the nondimensional time. Here, $\phi$ and $\tau$ are normalized as reference chord length and freestream velocity, respectively. In Eq. (1) $\xi$, $\eta$, and $\varsigma$ represent the axes in the computational domain, which correspond to $x$, $y$, and $z$ axes in the nondimensional physical coordinates of the streamwise, spanwise, and vertical directions, respectively. Several choices are available for the coefficients $F$, $G$, and $H$, depending upon the assumptions used in deriving the TSD equation. In the present study, the coefficients are defined as

$$
F = -\tfrac{1}{2}(\gamma + 1)M^2, \qquad G = \tfrac{1}{2}(\gamma - 3)M^2
$$

$$
H = -(\gamma - 1)M^2 \tag{2}
$$

The linear potential equation in the subsonic region can be recovered by simply setting $F$, $G$, and $H$ equal to zero. Equation (1) is solved using a time-accurate approximate factorization (AF) algorithm developed by Batina.[4] The AF algorithm consists of a time-linearization procedure coupled with a Newton iteration technique. An advanced Engquist–Osher type-dependent mixed difference operator[5,6] has been also implemented in the present AF algorithm to achieve the numerical stability in the supersonic flow regions. The applied boundary conditions of wing, pylon, and wake region are very similar to the method presented in Ref. 6. Modified slender body approximation technique on the store surfaces is applied effectively in this study, because the geometry of missile is quite slender. Nonreflecting far-field boundary conditions for more accurate and efficient unsteady calculations were used for both subsonic and supersonic inflow conditions. More detailed theoretical background and validation for the present study for the clean wing and wing with control surface can be seen in Ref. 7. The calculated results presented in Ref. 7 show a very good agreement with available experimental pressure data and previous analysis results.

## Results

Figure 1 shows the configuration of the wind-tunnel model of Northrop F-5 fighter wing with underpylon/launcher/missile and the corresponding surface grid for the present analysis. In this analytical study the pylon, launcher, and missile configurations including wing are entirely considered except the missile fins. Grid systems used in this study are first stretched at the missile and launcher nose and also at the leading and trailing edge of wing and underpylon. In the supersonic computation the grid qualities on the complex wing geometry play a more important role for safe convergence of steady calculation and run of unsteady calculation.

The comparisons of steady aerodynamic results in the transonic and low-supersonic flow region are presented in Fig. 2. In general, attaching a pylon and store under a wing has considerable effect on the flowfield because of blockage of the side flow. So, there are large variations of pressure distribution on the lower wing surface near the pylon. Moreover, at Mach number of 0.9, there are some discrepancies in the region of the pylon trailing edge because there are unexpected expansion shock waves numerically caused by the inviscid solution in this case. However, the overall trends between the experimental data and present results are very similar as shown in Fig. 2. In the supersonic Mach number of 1.33, the present results show the excellent agreements with the experimental data and also in the subsonic region although they are not presented in this Note. The steady-state solutions are normally converged within 500 iterations. There are large variations of the pressure distribution on the lower wing surface caused by the strong shock interaction between the wing and attached underpylon. Actually, in the subsonic region only small influences of pylon effect are shown because there

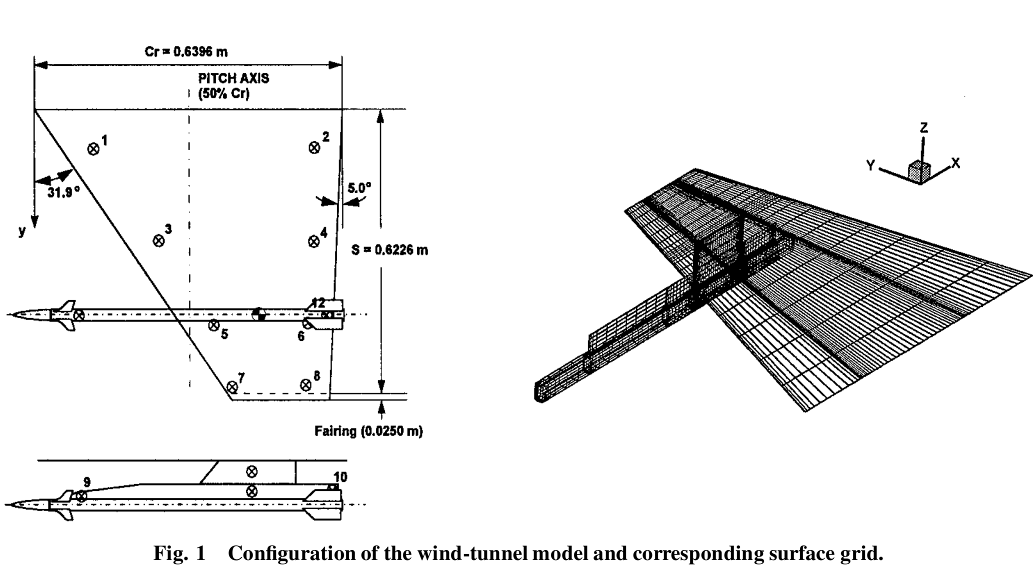


**Fig. 1 Configuration of the wind-tunnel model and corresponding surface grid.**

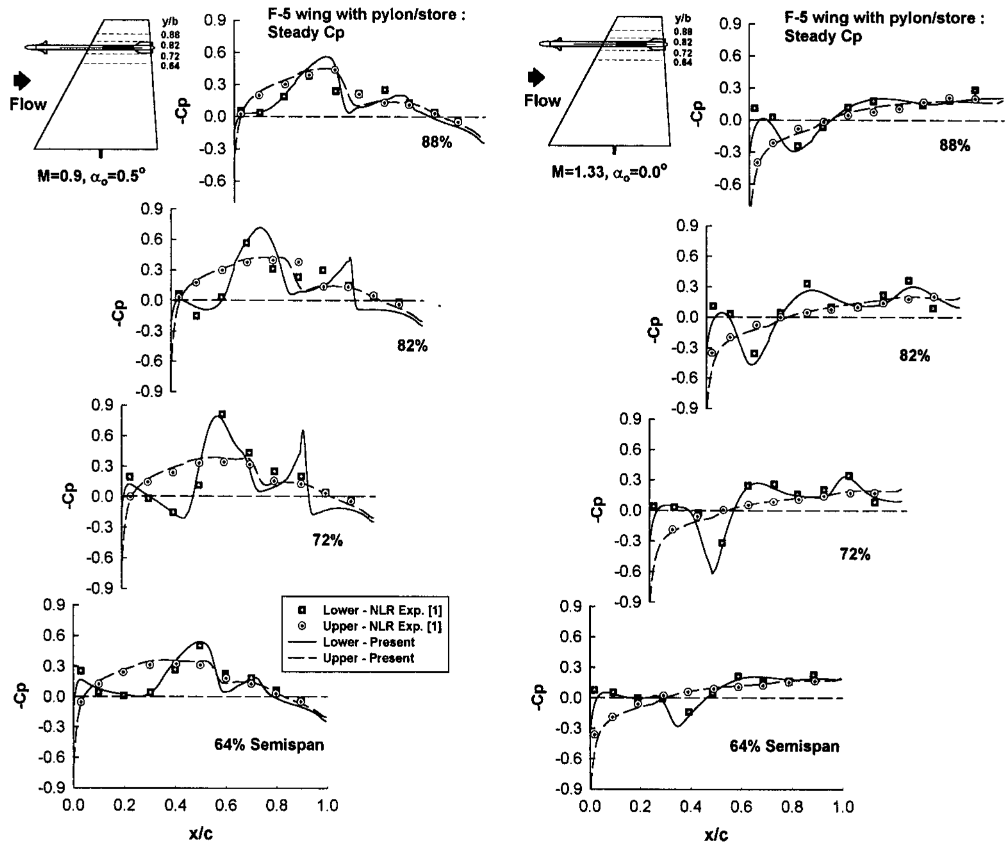


Fig. 2 Steady pressure comparisons between computation and experiment.

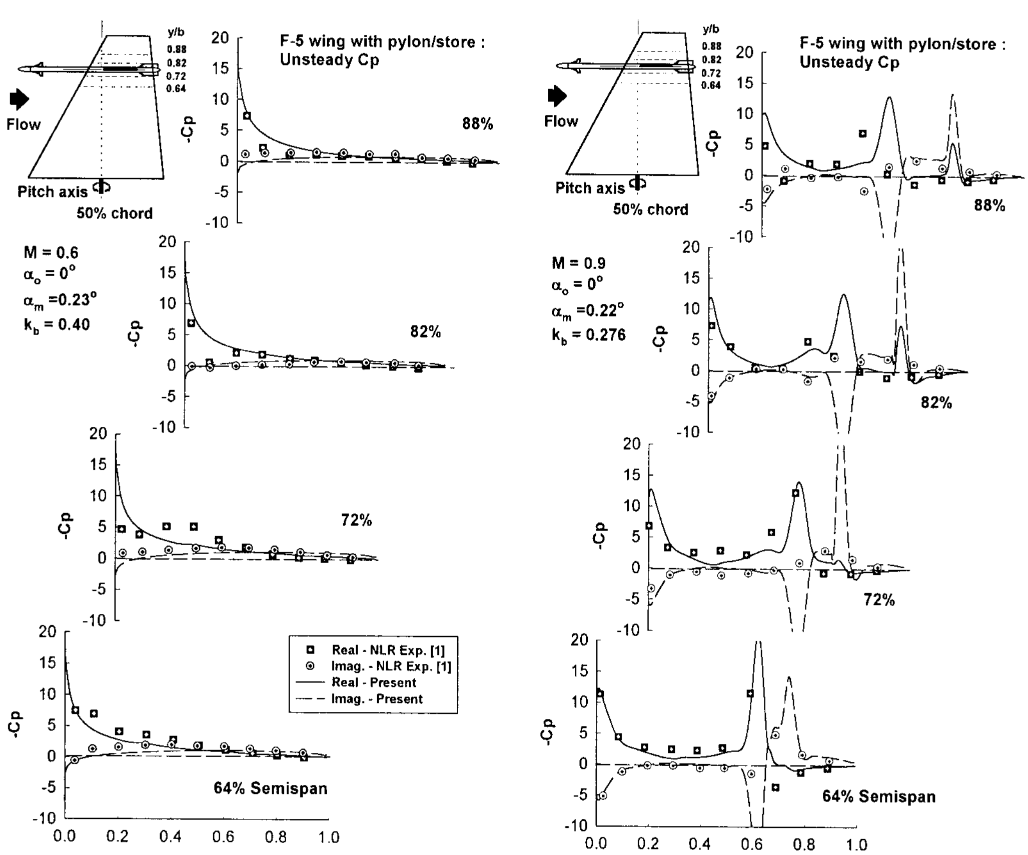


Fig. 3 Unsteady lower-surface pressure comparisons between computation and experiment.

are no shock waves. This phenomenon also can be seen from the experimental and linear analytical results of Ref. 1.

The unsteady aerodynamic comparisons are presented in Fig. 3. For unsteady calculations $10^{-5}$ order of maximum residual could be usually obtained by using just two subiterations in the inner Newton iteration process to increase the time accuracy. For the present unsteady calculation 720 time steps per cycle were normally performed using the grid system with the size of $105(x) \times 30(y) \times 51(z)$. The total elapsed time is about 930 s (user CPU time) during the three cycles using the f77 compile option of −O vector3 on the Cray-C90 computer at the System and Engineering Research Institute in the Republic of Korea. In Fig. 3 comparing with experimental results at Mach number of 0.9 expecting the strong shock and viscous interaction, we can also see that in the unsteady pressure distributions there are some discrepancies at near pylon stations because of the unexpected sharp inviscid shock waves. However, the overall trends of the present results are in a good agreement with the experiments. More detailed research including viscous effects will be requested in the future research. In the totally subsonic flow region expecting no shock interactions such as Mach number of 0.6, the present result given in Fig. 3 shows the very good agreement with the NLR's experimental data of Ref. 1.

## Conclusions

The present study has demonstrated the applicability of the TSD3KR code to the real aircraft wing such as F-5 fighter model in the transonic and low-supersonic flow region. In this study a more refined grid system was applied to the underpylon/store. The present results are directly compared with the wind-tunnel experiments of the NLR in transonic and supersonic flow regions. These results show good agreements with experimental steady and unsteady pressure distributions of the F-5 wing model. There are unexpected strong shock effects in the pressure distributions on the lower wing surface near the pylon trailing edge in the case of inviscid analysis.

## References

[1] Tijdeman, H., van Nunen, J. W. G., Kraan, A. N., Persoon, A. J., Poestkoke, R., Roos, R., Schippers, P., and Siebert, C. M., "Transonic Wind Tunnel Tests on an Oscillating Wing with External Stores; Parts I-IV," National Aerospace Lab. of The Netherlands, NLR-TR-78106, AFFDL-TR-78-194, 1978.

[2] Guruswamy, G. P., and Goorjian, P. M., "An Efficient Coordinate Transformation Technique for Unsteady, Transonic Aerodynamic Analysis of Low Aspect-Ratio Wings," *Journal of Aircraft*, Vol. 22, No. 3, 1985, pp. 193–199.

[3] Guruswamy, G. P., Goorjian, P. M., and Tu, E. L., "Unsteady Transonics of a Wing with Tip Store," *Journal of Aircraft*, Vol. 23, No. 8, 1986, pp. 662–668.

[4] Batina, J. T., "Efficient Algorithm for Solution of the Unsteady Transonic Small-Disturbance Equation," *Journal of Aircraft*, Vol. 25, No. 10, 1988, pp. 962–968.

[5] Batina, J. T., "Unsteady Transonic Algorithm Improvements for Realistic Aircraft Applications," *Journal of Aircraft*, Vol. 26, No. 2, 1989, pp. 131–139.

[6] Engquist, B. E., and Osher, S. J., "Stable and Entropy Satisfying Approximations for Transonic Flow Calculations," *Mathematics of Computation*, Vol. 34, No. 149, Jan. 1980, pp. 45–75.

[7] Kim, D. H., Ji, S. G., Lee, I., and Kwon, J. H., "Transonic Aerodynamic Analysis Using Transonic Small Disturbance Equation," *Journal of the Korean Society for Aeronautical and Space Sciences*, Vol. 26, No. 2, 1998, pp. 1–9.